

A Simple New Way To Account for Free Volume in Glassy Dynamics: Model-Free Estimation of the Close-Packed Volume from PVT Data

Ronald P. White and Jane E. G. Lipson*



Cite This: <https://doi.org/10.1021/acs.jpcb.1c01620>



Read Online

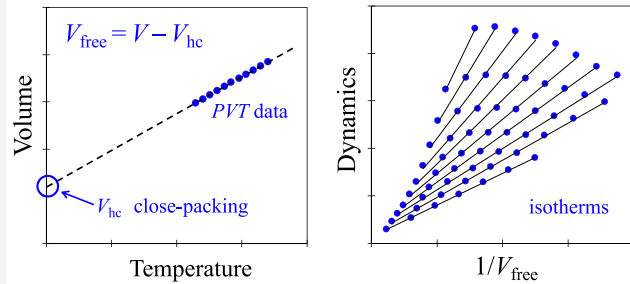
ACCESS |

Metrics & More

Article Recommendations

Supporting Information

ABSTRACT: In this article we focus on the important role of well-defined free volume (V_{free}) in dictating the structural relaxation times, τ , of glass-forming liquids and polymer melts. Our definition of $V_{\text{free}} = V - V_{\text{hc}}$, where V is the total system volume, means the use of V_{free} depends on determination of V_{hc} , the system's volume in the limiting closely packed state. Rejecting the historically compromised use of V_{free} as a dynamics-dependent fitting function, we have successfully applied a clear thermodynamics-based route to V_{hc} using the locally correlated lattice (LCL) model equation of state (EOS). However, in this work we go further and show that V_{hc} can be defined without the use of an equation of state by direct linear extrapolation of a $V(T)$ high-pressure isobar down to zero temperature (T). The results from this route, tested on a dozen experimental systems, yield $\ln \tau$ vs $1/V_{\text{free}}$ isotherms that are linear with T -dependent slopes, consistent with the general $\ln \tau \sim f(T) \times (1/V_{\text{free}})$ form of behavior we have previously described. This functional form also results by implementing a simple mechanistic explanation via the cooperative free volume (CFV) rate model, which assumes that dynamic relaxation is both thermally activated and that it requires molecular segmental cooperativity. With the degree of the latter, and thus the activation energy, being determined by the availability of free volume, the new route we demonstrate here for determination of V_{free} expands the potential for understanding and predicting local dynamic relaxation in glass-forming materials.



1. INTRODUCTION

Over the past several decades, there has been robust interest in how the dynamics in liquids change, slowing and ultimately ceasing, as they approach their glass transition.^{1–14} For many polymers and small molecule glass formers, as temperature (T) is lowered under ambient conditions, dynamic quantities such as structural/segmental relaxation times (τ), viscosity (η), diffusion coefficients (D), and related properties will exhibit non-Arrhenius behavior. That is, $\ln \tau$, $\ln \eta$, $-\ln D$, etc., are not linear in $1/T$, but rather show system-dependent degrees of upward curvature (i.e., fragility^{8,15}). Some of the explanations for this behavior focused on “free volume”, as defined by the Doolittle equation,^{16–19} being the controlling factor in glassy dynamics. In this picture a rather extreme assumption was made: that dynamics depend on free volume alone.

These older free volume models^{17–19} had some success but only for data sets under ambient isobaric conditions. In addition to their failure under changing pressure, a key criticism was that the definition of “free volume” did not map directly to a liquid’s actual volumetric data. For example, these models assumed the existence of a finite temperature (T_0) where free volume would “disappear”. Further, they did not provide a route to this limiting temperature via thermodynamic (volumetric) measurements but instead required that it be determined *a posteriori* (fit) from the dynamics results. This guaranteed that the model would follow the phenomenological

VFT $\ln \tau \sim 1/(T - T_0)$ form^{20–22} (mathematically equivalent to the form of the free volume-based WLF equation¹⁷). While the VFT functional form is able to fit ambient pressure dynamics data, the lack of theoretical underpinning means that it cannot illuminate the connection between volume and dynamics.

As experimental data accrued for conditions under which both pressure and temperature were varied (pressure-dependent dynamics^{1,2}), the limits of historical free volume models became even more apparent. These experiments clearly showed that dynamics change with T even when the volume, therefore the “free volume”, is fixed. Use of the Doolittle description in such cases requires transforming the free volume into what essentially becomes a fitting function. For more background on the history of free volume and its various definitions, we direct the interested reader to ref 23. Despite the historical baggage associated with earlier definitions, the notion of local space (aka “free volume”) being required to

Received: February 22, 2021

Revised: March 26, 2021

enable local relaxation retains sensible appeal. However, it is clear that free volume cannot be the only important variable upon which dynamic behavior depends.

As noted above, pressure-dependent experiments show that relaxation times, $\tau(T,V)$, depend on *independent* contributions from both temperature and volume.^{1,2} In recent work^{24–29} we have demonstrated that volume and free volume can be connected in a fundamental and well-defined manner by calculating V_{free} for experimental systems based on pressure, volume, temperature (PVT) data, and equation of state analysis. Further, we have found that free volume is one of the *natural* variables that leads to analytic analysis of dynamic relaxation data, the other being temperature. In particular, we showed for the first time,²⁷ that *isotherms* of $\ln \tau$ when plotted against $1/V_{\text{free}}$ are linear, with slopes that increase with decreasing T . Our mechanistic derivation of the resulting functional form, *viz.*, $\ln \tau \sim f(T) \times (1/V_{\text{free}})$, leads to the cooperative free volume rate model^{24–26} (CFV). This analysis begins with the view of segmental motion as a relaxation process that is both thermally activated and cooperative, with the latter being dictated by the availability of free space. Additional detail is provided below.

In this new work we introduce a very simple, physically transparent way to evaluate the free volume *directly* from pressure, volume, temperature (PVT) data. We emphasize that this route, in contrast to our previous applications to experimental systems, does not require translation through a theoretical equation of state to assign the volume at close-packing. We then demonstrate for a dozen different materials that this experimentally determined free volume (along with temperature) leads to illuminating analyses of dynamic relaxation data over a wide range of T and P . Our larger goal, by way of these examples, is both to show how dynamics can be explained in terms of independent, thermodynamically defined, physical properties and to strengthen interest in free volume as a fundamental physical quantity.

2. DEFINITION AND CALCULATION OF FREE VOLUME

A meaningful connection between dynamics and free volume requires that it be defined independently of the dynamics, using only thermodynamic data (*i.e.*, PVT data). Our definition is

$$V_{\text{free}}(T,P) = V(T,P) - V_{\text{hc}} \quad (1)$$

$V_{\text{free}}(T,P)$ at any T,P is simply the difference between the system's total volume, $V(T,P)$, and the volume of its close-packed state, V_{hc} .

In most of our work up to now, we have evaluated V_{hc} by applying the locally correlated lattice model (LCL) equation of state (EOS) to the analysis of experimental PVT data.^{23,30} LCL is a theoretical EOS with molecular parameters yielding a well-defined model interpretation of the system's characteristic volume at close-packing (V_{hc}). The LCL equation is given by

$$\begin{aligned} \frac{P}{k_B T} = & \left(\frac{1}{v} \right) \ln \left[\frac{V}{V - N_m r v} \right] \\ & + \left(\frac{3}{v} \right) \ln \left[\frac{V - (N_m v/3)(r - 1)}{V} \right] \\ & - \left(\frac{3}{v} \right) \left(\frac{(2r + 1)^2}{(V/N_m v) - (1/3)(r - 1)} \right) \\ & \times \left(\frac{\exp[-\epsilon/k_B T] - 1}{(1/3)(2r + 1)\exp[-\epsilon/k_B T] + (V/N_m v) - r} \right) \end{aligned} \quad (2)$$

where k_B is the Boltzmann constant. The molecular parameters are r , the number of segments (occupied lattice sites) per molecule, v , the volume per lattice site, and ϵ , the segment–segment nonbonded interaction energy. The model fluid contains both occupied and unoccupied lattice sites (making it compressible); rv is the theoretical volume of a single molecule. In eq 2, N_m is the total number of molecules, and therefore $N_m r$ is the total number of molecular segments. (In practice, either the volume per molecule, V/N_m , or, given the molecular weight, the volume per mass, can be used as a convenient intensive input variable.) The route to V_{free} involves fitting the LCL EOS to PVT data to obtain the three parameters, r, v, ϵ . The volume at close-packing is $V_{\text{hc}} = N_m r v$, and this is used in eq 1, for example, to evaluate V_{free} at the T,P conditions of specific experimental dynamics datum points. We have shown for many systems^{24,27,31} that this thermodynamic route to V_{free} leads to linear $\ln \tau$ vs $1/V_{\text{free}}$ isotherms with T -dependent slopes.

One procedural caveat^{24,28,31} associated with the LCL-based approach is that, for self-consistency, calculation of $V_{\text{free}}(T,P) = V(T,P) - V_{\text{hc}}$ should be undertaken using the LCL V_{hc} in conjunction with the *fitted* theoretical LCL $V(T,P)$. In fact, inside the LCL (T,P) data fitting range (we typically fit over 0 to 100 MPa) the true experimental $V(T,P)$ value and the fitted LCL $V(T,P)$ value are essentially the same, and this caution is irrelevant. However, it may be that dynamic data of interest fall outside the range of experimental PVT results (*e.g.*, above 200, 300 MPa), and under those conditions the LCL prediction for $V(T,P)$ will deviate from the experimental data (for example in systems we have checked, at 100 to 200 MPa beyond the LCL fitting range the theoretical estimates for $V(T,P)$ might be off by up to 1–2%). This difference arises because the simple LCL model has only three adjustable parameters, which limits the range it can capture. It turns out that taking the difference between the LCL $V(T,P)$ and the corresponding LCL V_{hc} provides internal consistency and leads to cancellation of errors. The result, illustrated in many successful applications^{24,27,27} and discussed further below, is that the LCL free volume analysis can be extended to a range of dynamics data much wider than the LCL PVT data fitting range.

There are other equations of state that work over a wider range by using more parameters. One example is the widely used phenomenological Tait equation

$$V(T,P) = V(0,T) \times \{1 - C \ln[1 + P/B(T)]\}$$

$$\text{where } V(0, T) = A_0 + A_1 T + A_2 T^2$$

$$\text{and } B(T) = B_0 \exp(-B_1 T)$$

(3)

Note that in keeping with common practice, temperature in the Tait EOS is applied in units of $^{\circ}\text{C}$. (In all other cases we apply T in units of K.) The five parameters, A_0 , A_2 , A_3 , B_0 , B_1 , are fit to *PVT* data, with a fixed value assumed for C prior to fitting, e.g., it is commonly, but not always, set at $C = 0.0894$. (A four-parameter version of the Tait equation is also available, incorporating an exponential rather than quadratic T -dependence.) A good description of implementations of the Tait equation is provided in the work by Yi and Zoller.³²

However, while the five adjustable parameters (two more than LCL) of the Tait equation lead to a good fit over a wider range, it is not a molecularly based theoretical equation, and it does not predict a corresponding closed-packed volume. Note that use of the Tait $V(T,P)$ in combination with an LCL V_{hc} would lead to the same problem as described above by using an experimental $V(T,P)$ from outside the LCL fitting range. This means that in order to use the more accurate Tait $V(T,P)$ values in eq 1, we still need a route to determine an appropriate corresponding V_{hc} for the case in which a very wide range of (T,P) conditions—say, for data spanning hundreds of MPa—are of interest. This is what we turn to next.

3. NEW ROUTE TO THE VOLUME AT CLOSE-PACKING

We now describe an alternative route to V_{free} that is *PVT* data-based and still uses the simple eq 1 definition, $V_{\text{free}}(T,P) = V(T,P) - V_{\text{hc}}$. Here the close-packed volume, V_{hc} , is estimated in a way that does not require translation through the LCL (or any other) theoretical equation of state and can be applied together with $V(T,P)$ values which are experimentally accurate over a very wide range (i.e., wider than LCL). In particular, we will be able to apply eq 1 using the more accurate $V(T,P)$ from fits of the empirical Tait equation.

The method for obtaining V_{hc} involves extrapolating $V(T)$ isobars from *PVT* data down to the value at $T = 0$. We have previously demonstrated the feasibility of this approach with two simulated systems:^{25,26} the monomeric Kob and Andersen Lennard-Jones (KA-LJ) mixed fluid²⁵ and a fluid melt of Lennard-Jones bead-spring model polymers.²⁶ In those works, the range of volume values in the simulated *PVT* data was far too wide to consider fitting with the LCL EOS. Instead, we used the portions of $V(T)$ where T was low enough for the data to be linear and extrapolated the simulated isobars down to $T = 0$ to obtain a sensible estimate of V_{hc} . We used the resulting V_{hc} value (the best single compromise value considering several isobars at different pressures) in eq 1 along with the exact simulated volume, $V(T,P)$, to calculate $V_{\text{free}}(T,P)$. Using these results for the abscissa, we found, once again, isotherms of $\ln \tau$ vs $1/V_{\text{free}}$ to be linear, with slopes that increased with decreasing T .

In that work,^{25,26} because model Lennard-Jones atoms have a simple spherical shape, we also verified that the V_{hc} we obtained connected sensibly to the volume at close-packing. As T decreases toward zero, it is reasonable to expect that (if the glass transition did not intervene) the equilibrium amorphous liquid must be tending toward a state of random (and not crystal) close packing. This state has for example a packing fraction of 0.64 for equal sized spheres; for mixed spheres, the value should be a little higher. Our extrapolated V_{hc} for the KA-LJ mixture corresponded to a packing fraction of 0.67 which is very close to this range (for more details, see refs 25 and 26).

In the simulation work, the estimated uncertainty in extrapolating V_{hc} was roughly $\pm 3\%$. Our tests verified that

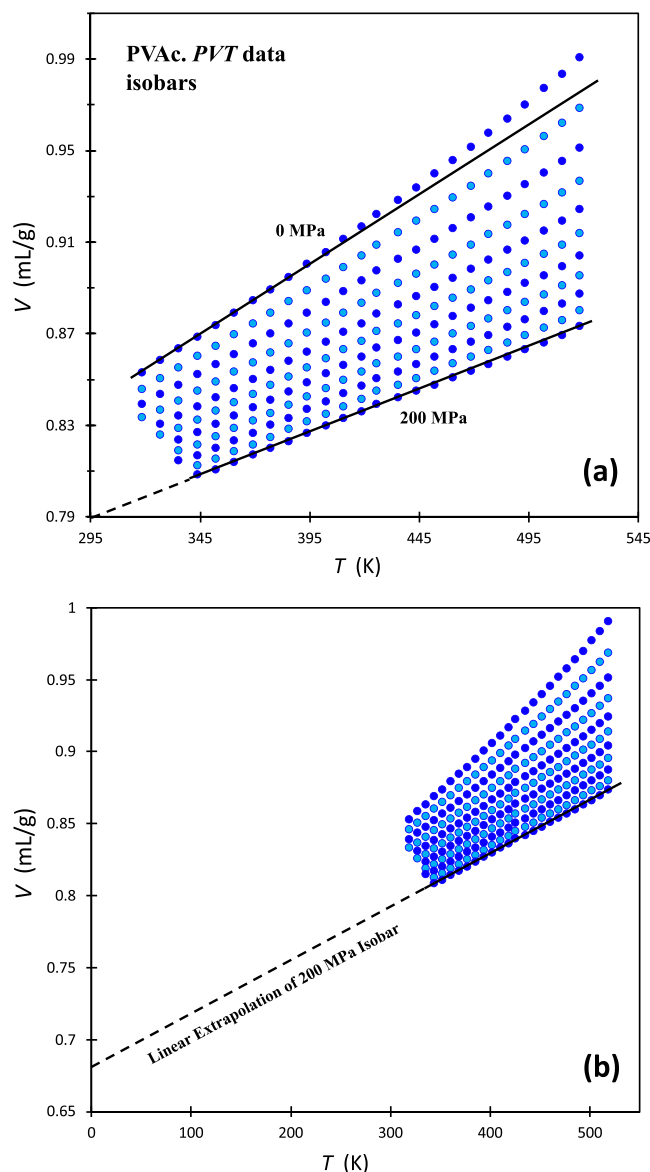


Figure 1. Poly(vinyl acetate) (PVAc) *PVT* data from Zoller and Walsh.³³ Panel a shows $V(T)$ isobars at pressure values of 0, 20, 40, 60, 80, 100, 120, 140, 160, 180, 200 MPa. The lines demonstrate the typical curvature of the low pressure $V(T)$ isobars (e.g., 0 MPa) and the typical linearity of the higher pressure $V(T)$ isobars (e.g., 200 MPa). Panel b has the same *PVT* data displayed on a scale showing the linear extrapolation of the 200 MPa $V(T)$ isobar down to $T = 0$; this extrapolated value (~ 0.68 mL/g) provides an approximation for the PVAc volume at close-packing.

using V_{hc} values anywhere within this range to calculate V_{free} led to isothermal plots of $\ln \tau$ vs $1/V_{\text{free}}$ that were linear with T -dependent slopes. We have also confirmed that taking values outside of the uncertainty range, e.g., values that visual judgment show lie outside the range of linear extrapolation, will not lead to linear $\ln \tau$ vs $1/V_{\text{free}}$ isotherms. The implication is that there is a “sensible” range of V_{hc} values that will lead to V_{free} predictions that strongly correlate with independent dynamics data. However, this range is not endlessly elastic; unphysical values for V_{hc} will prevent meaningful analysis of dynamic data. Our conclusions regarding the simulated systems also apply to the experimental results presented here.

Table 1. System Acronyms, V_{hc} Values, and References to Experimental Dynamics and PVT Data

acronym	name	lower bound V_{hc} (mL/g)	best value V_{hc} (mL/g)	data $\tau(T,P)$	data PVT
PVAc (polymeric liquid)	poly(vinyl acetate)	0.6812	0.7017	34, 35	33
PVME (polymeric liquid)	polyvinylmethyl ether	0.7920	0.8158	36	37
PMPS (polymeric liquid)	polymethylphenylsiloxane	0.7497	0.7722	38	39
PMTS (polymeric liquid)	polymethyltolylsiloxane	0.6510	0.6705	40	39
PPMA (polymeric liquid)	polypropyl methacrylate	0.7750	0.7983	41	33
NR (polymeric liquid)	natural rubber	0.9056	0.9327	42	33
PU (polymeric liquid)	polyurea	0.7569	0.7796	43	43
PDE (molecular liquid)	phenolphthalein dimethyl ether	0.5926	0.6103	44	45
BMPC (molecular liquid)	1,1'-bis(<i>p</i> -methoxyphenyl)cyclohexane	0.7265	0.7483	46	47, 48
BMMPC (molecular liquid)	1,1'-bis(4-methoxy-5-methylphenyl)cyclohexane	0.7686	0.7917	49	47, 48
BMP-BOB (ionic liquid (IL))	1-butyl-1-methylpyrrolidinium bis[oxalate]borate	0.6486	0.6681	50	51
TPIL (polymerized IL)	poly(3-methyl-1,2,3-triazolium bis(trifluoromethylsulfonyl)imide)	0.6025	0.6206	52	52

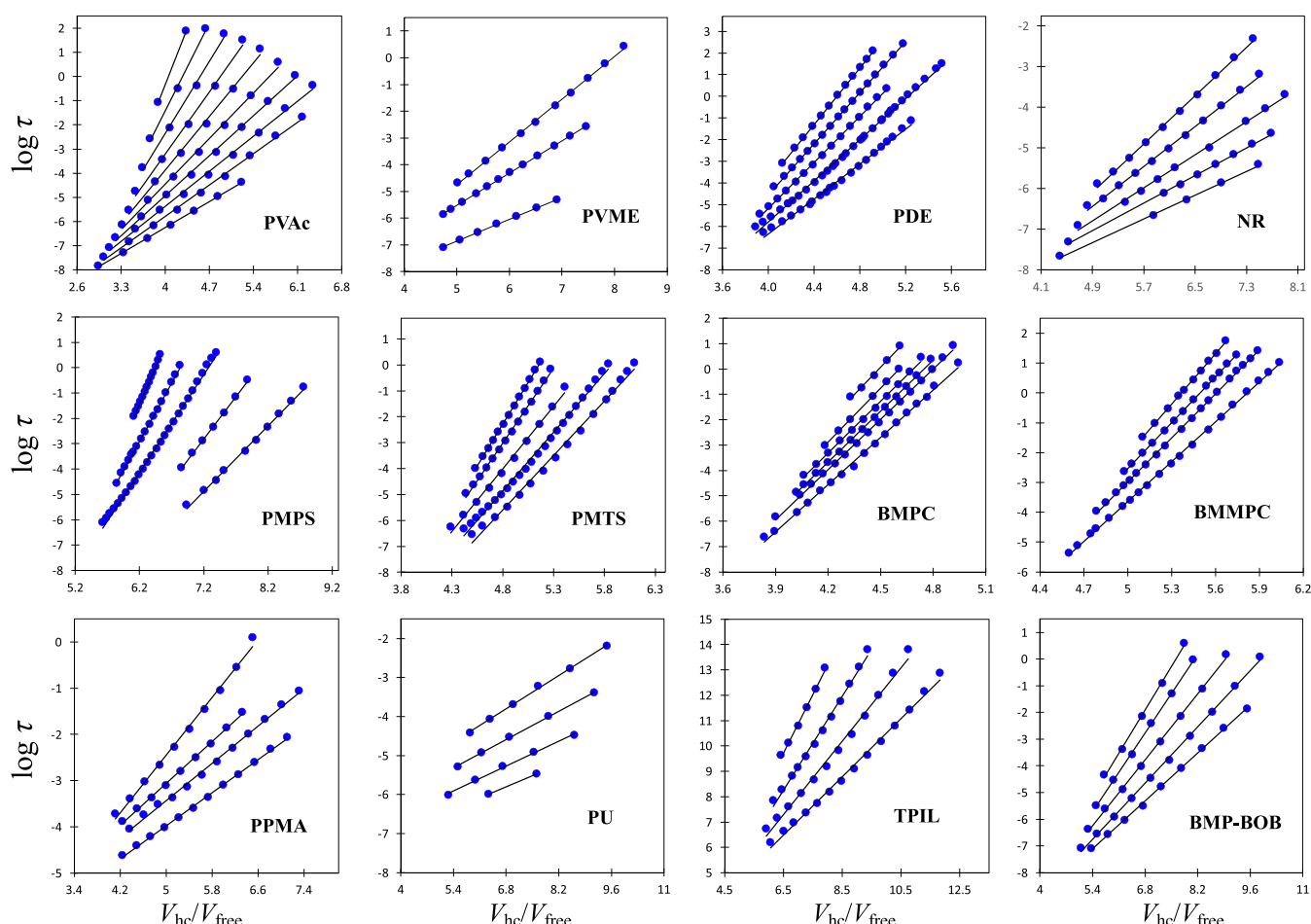


Figure 2. T,P -dependent α -relaxation times (τ) plotted as $\log \tau$ vs V_{hc}/V_{free} isotherms, for polymer and small molecule liquids. Symbols mark each experimental relaxation time at the corresponding V_{hc}/V_{free} value, and the lines are the corresponding linear fits. Here $V_{\text{free}}(T,P) = V(T,P) - V_{hc}$ is calculated based on PVT data using the linearly extrapolated $V(T=0, P=200 \text{ MPa})$ value to define V_{hc} (the lower bound estimate of V_{hc}). Systems include the following: PVAc, PVME, PDE, NR, PMPS, PMTS, BMPC, BMMPC, PPMA, PU, TPIL, and BMP-BOB. (In the one case of TPIL, \log of DC conductivity is plotted on the ordinate.) Typically for most systems, the dynamics data points cover pressure ranges from $P = 1 \text{ atm}$ (0.1 MPa) to roughly around 200 MPa and in some cases to 300 or 400 MPa. Temperature values varied with system and are available in the experimental references. As one specific example, for the case of PVAc, the isotherm temperatures ranged from 323 K (top line) to 413 K (bottom line) in increments of 10 degrees, and pressure values ranged from 0.1 MPa (in 50 MPa increments) up to as high as 400 MPa. System acronyms, V_{hc} values, and references for experimental PVT and dynamics (dielectric spectroscopy) data are available in Table 1.

Figure 1 shows PVT data for poly(vinyl acetate) (PVAc). In Figure 1a, the plots are $V(T)$ isobars, ranging from $P = 0$ ($\approx 1 \text{ atm}$) to 200 MPa in increments of 20 MPa. Note that the

isobars at lower pressure exhibit systematic positive curvature (e.g., see the line drawn at the $P = 0$ isobar), a phenomenon commonly seen in other systems. Some system data sets may

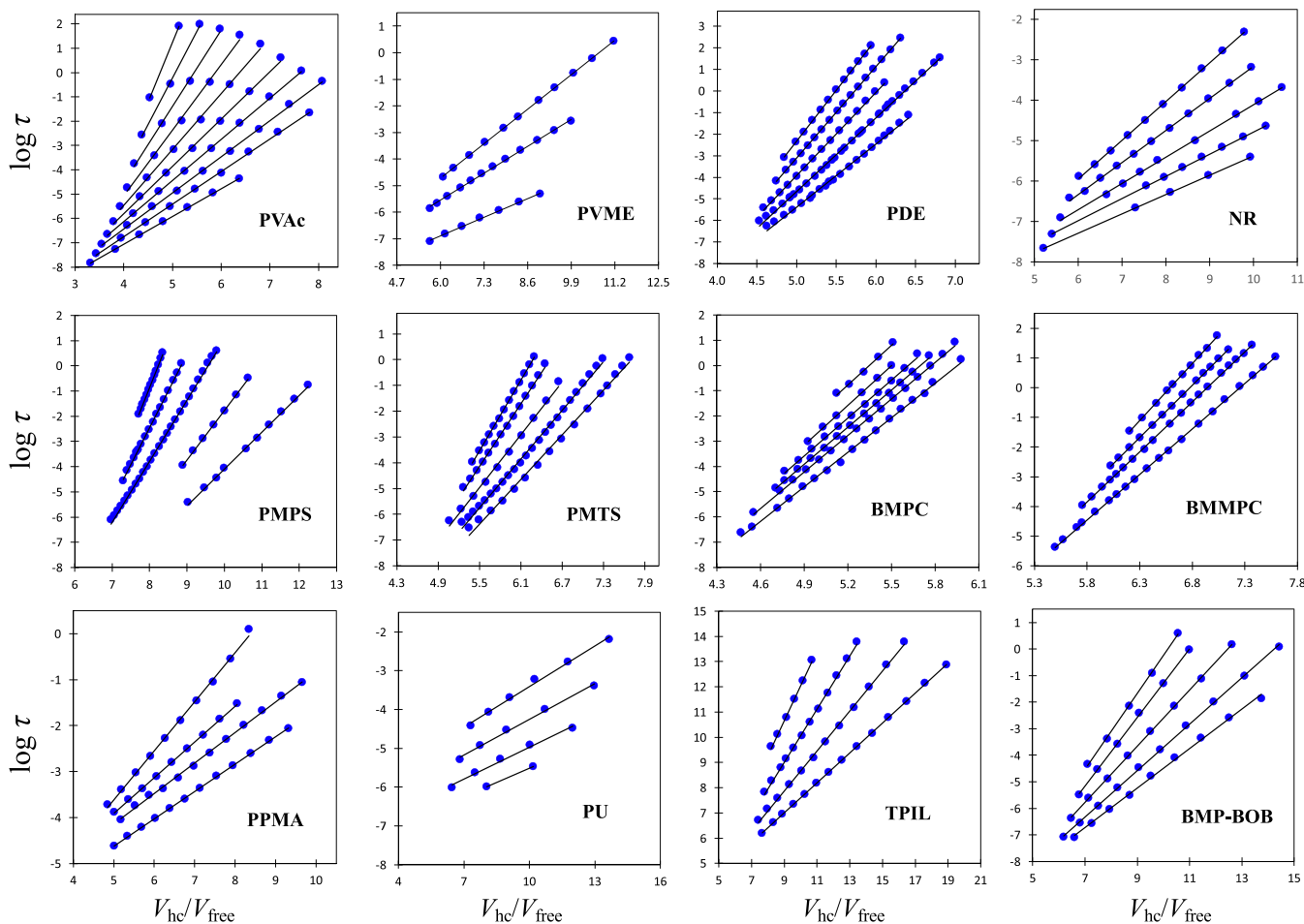


Figure 3. T,P -dependent α -relaxation times (τ) plotted as $\log \tau$ vs $V_{\text{hc}}/V_{\text{free}}$ isotherms, for polymer and small molecule liquids. Symbols mark each experimental relaxation time at the corresponding $V_{\text{hc}}/V_{\text{free}}$ value, and the lines are the corresponding linear fits. Here $V_{\text{free}}(T,P) = V(T,P) - V_{\text{hc}}$ is calculated based on PVT data using the best estimate for V_{hc} , which is equal to the linearly extrapolated $V(T=0,P=200 \text{ MPa})$ lower bound value with a +3% correction. For additional system details, refer to the caption of Figure 2 and Table 1.

show more linear low pressure isobars, while in other data sets, especially at higher temperature ranges, there may be even more upward curvature. In contrast, the isobars at higher pressure are reliably linear for all systems. In Figure 1a, a line has been drawn through the data for the 200 MPa $V(T)$ isobar.

In PVT experiments, for example using a Gnomix apparatus,^{32,33} it is common to take measurements up to 200 MPa, so we choose to focus on this particular isobar in prescribing a procedure for linear extrapolation of volume to $T = 0$. While the choice of 200 MPa is somewhat arbitrary, it protects from the potential error in choosing a lower pressure where there might be a small amount of curvature. However, we observe that choosing any other nearby pressures associated with a linear plot will only change the results by a small amount and will not affect the conclusions.

Figure 1b implements this simple procedure, showing the linear extrapolation of the PVAc 200 MPa $V(T)$ isobar down to $T = 0$; the value obtained is 0.681 mL/g. This is a sensible *lower bound* estimate for the close-packed volume, V_{hc} (more on this further below). We have similarly obtained the linearly extrapolated $V(T=0,P=200 \text{ MPa})$ values for 11 other polymer and small molecule glass-forming liquids. The linear $V(T)$ fits for all systems are shown in the Supporting Information (SI), and the resulting V_{hc} values (i.e., the linear intercepts) are summarized in Table 1. Next we apply these

lower bound estimates for V_{hc} in eq 1, and test the correlation of the resulting V_{free} values with dynamics data.

4. CORRELATION BETWEEN FREE VOLUME AND DYNAMICS

Figure 2 shows results using the route described above for V_{free} , applied to 12 systems, including polymers and glass-forming molecular liquids, as well as an ionic liquid and a polymerized ionic liquid. For each system, the pressure-dependent dynamics results (α relaxation times measured by dielectric spectroscopy) are plotted in the form of $\ln \tau$ vs $1/V_{\text{free}}$ isotherms. To ensure internal consistency, we obtained the $V(T,P)$ values for use in eq 1, at each dynamics T,P data point via the Tait equation fitted to the corresponding experimental PVT data. These $V(T,P)$ values are expected to be very accurate, even where in some cases the dynamics data are extending to pressures of 300 MPa or higher. (Values for all the Tait EOS parameters are available in the SI.) The results in Figure 2 demonstrate that using $V_{\text{free}}(T,P)$ values obtained as described above leads to the anticipated strong correlation with dynamic relaxation data. The $\ln \tau$ vs $1/V_{\text{free}}$ isotherms are for the most part linear and show T -dependent slopes, the same basic trends we had already shown^{24,27,31} using the LCL EOS analysis to define V_{free} for the same experimental systems.

In section 3 we said that we expect the linearly extrapolated $V(T = 0, P = 200 \text{ MPa})$ value to be a lower bound estimate for V_{hc} for the range of the given PVT data. The reason for this is that an accurate extrapolation of a $V(T)$ isobar at lower pressure (if curvature could be hypothetically accounted for) would yield a V_{hc} greater than our lower bound. It is sensible even despite the uncertainty in accounting for its curvature to expect that the $P = 1 \text{ atm}$ $V(T)$ isobar will extrapolate to a value at $T = 0$ that should not be much more than about 5% above the corresponding value for the $P = 200 \text{ MPa}$ isobar. Because there is no reason to preference an extrapolated value at one pressure over another, this suggests using an averaged value that we can estimate by taking as 2–3% larger than the clearly linear extrapolation at 200 MPa yields.

Our procedure for obtaining V_{hc} directly from experimental PVT data for a material of interest (termed the “best value” in Table 1) is therefore to determine the lower bound value by extrapolating the $V(T, P = 200 \text{ MPa})$ plot to $T = 0$ and then applying a +3% correction. We take this result for V_{hc} to be constant for that substance in all following analysis.

Using the corrected values of V_{hc} , we recalculated V_{free} results and reanalyzed the dynamics data for all 12 systems. The results are shown in Figure 3 where we see, again, that for each system the isotherms are linear with T -dependent slopes.

Comparison between the Figure 2 and Figure 3 results shows that having an uncertainty in V_{hc} of about 3% percent is acceptable for V_{free} analysis using eq 1, and this is important because this model-free route to V_{hc} involves approximation. From a more fine-grained perspective it appears that, on average, the linearity of the Figure 3 $\ln \tau$ vs $1/V_{\text{free}}$ isotherms is a little stronger than that in Figure 2. (Average correlation coefficients are $R^2 = 0.9976$ and 0.9984 for the results in Figures 2 and 3, respectively.) In particular, the isotherms of Figure 2 are more likely to show a slight positive curvature compared to those in Figure 3. We have found²⁵ that positive curvature develops if using a V_{hc} that is a too small, and so this is consistent with the Figure 2 V_{hc} values being lower bound approximations.

In closing this section, it is important to emphasize that, both in all our previous studies and in this work, the $\ln \tau$ vs $1/V_{\text{free}}$ plots have abscissa values that are based on thermodynamic data, alone, while the ordinate values are from dynamic data, alone. These linear plots clearly illustrate the strong connection linking thermodynamic and dynamic behavior. To further illustrate this point, we can connect with the results in the recent Cheng et al.⁵³ investigation of free volume in TPIL, which employed the accurate Tait EOS for $V(T, P)$. In that work, the authors *assumed* the validity of our CFV prediction that *isotherms* of $\ln \tau$ data as a function of inverse free volume would be linear with T -dependent slopes (Figures 2 and 3). (Standard isobars of $\ln \tau$ vs $1/V_{\text{free}}$ are not linear as was once believed; see below.) By taking the eq 1 definition of $V_{\text{free}}(T, P) = V(T, P) - V_{\text{hc}}$ but treating V_{hc} as an unknown, they fit the dynamics data to extract a V_{hc} value. Their fitted result for TPIL, $V_{\text{hc}} = 0.625 \text{ mL/g}$, closely matches the thermodynamically based result we include in this work of 0.621 mL/g. The close match between the value that the dynamics data would require and the value that the independent thermodynamic analysis would predict further validates the close connection between the two realms. That is, the fact that our analysis allows us to sensibly link a fit value of V_{hc} , extracted from dynamics data, to a quantity that is well-defined, with thermodynamic origins, provides the justification

for any approach whereby measurement of dynamics data might plausibly provide a different route to estimate V_{free} (i.e., to assume the $\ln \tau \sim f(T) \times (1/V_{\text{free}})$ form holds).

5. INSIGHT: WHY DYNAMICS FOLLOWS THE $\ln \tau \sim f(T) \times (1/V_{\text{free}})$ FORM

We now explain why $\ln \tau$ and the variable, $1/V_{\text{free}}$, form a linear relationship on isotherms and why the slopes of the isotherms increase with decreasing T . Note that these trends are consistent with the broader observations from pressure-dependent experiments,^{1,2} which show that dynamics have an independent contribution from both temperature and volume. In contrast, the Doolittle equation ($\tau = A \exp[B/V_{\text{free}}]$, where A and B are constants) assumes no independent contribution from temperature; if that were the case, then all $\ln \tau$ vs $1/V_{\text{free}}$ isotherms would fall on a single line, no T -dependence. The Doolittle picture does not just fail to capture isotherms, it also cannot capture experimental behavior on isobars, which is what we turn to next.

5.1. Temperature and Free Volume Both Play a Role on Isobars.

Historical Doolittle-based free volume models^{17–19} predict that the isobaric $\ln \tau$ vs $1/V_{\text{free}}$ trend must be linear. The results in Figure 4 show this is not the case; there is

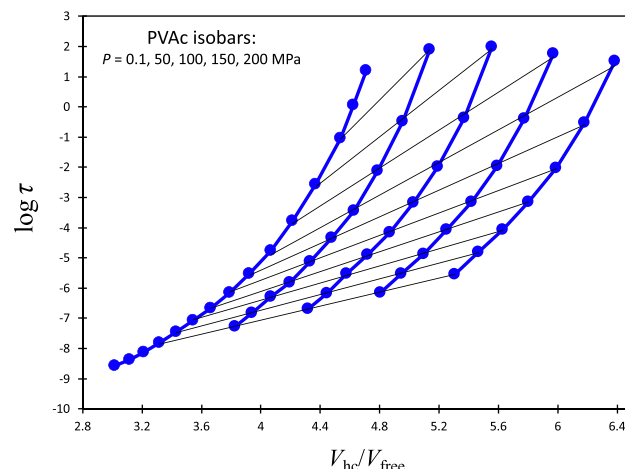


Figure 4. Poly(vinyl acetate) (PVAc) α -relaxation times (τ) plotted as $\log \tau$ vs $V_{\text{hc}}/V_{\text{free}}$ (PVT and dynamics data from refs^{33–35}). Isobars are indicated as the heavy curves (drawn as a guide to the eye); the standard ambient pressure isobar ($P = 0.1 \text{ MPa}$) is the leftmost curve and to its right are isobars at $P = 50, 100, 150$, and 200 MPa . The light lines drawn through the data indicate the corresponding linear isotherms ($T = 323, 333, 343, 353, 363, 373, 383, 393, 403, 413 \text{ K}$). In these results, $V_{\text{free}}(T, P) = V(T, P) - V_{\text{hc}}$ at each dynamics datum point is calculated based on PVT data as described in the text. While isotherms are linear, isobars show upward curvature due to the independent T -based contribution to dynamics; the isobaric trend is thus in contradiction to the predictions of Doolittle-based models; see text for details.

clear upward curvature. Here we used data for PVAc as an example; the ambient pressure isobar is the leftmost plot, and the curves to the right correspond to isobars at higher pressures. (For convenience in comparison, the corresponding linear isotherms have also been drawn through the same data.) The Doolittle prediction that all isobars would collapse to a single line does not hold.

In our work,²⁷ we demonstrated the nonlinearity of $\ln \tau$ vs $1/V_{\text{free}}$ on isobars using the LCL EOS definition for the close-

packed volume, V_{hc} . The results here, using the present model-free determination of V_{hc} , also support this conclusion. The source of the upward curvature can be traced to the independent contribution from temperature. In an isothermal plot only the volume changes; plotting $\ln \tau$ vs $1/V_{free}$ fully accounts for this volume dependence (the mechanistic reason for this is discussed below), so the slope of the plot remains constant. However, on an isobar the volume and temperature are both changing; the resulting upward curvature is caused by the multiplicative coupling of T and V contributions, which we explain below using the Cooperative Free Volume (CFV) rate model.

5.2. The Cooperative Free Volume Rate Model. The results from our recent studies have clearly demonstrated that free volume is a natural variable for describing dynamics, with temperature as the other variable. We have developed the cooperative free volume (CFV) rate model²⁵ to provide a simple theoretical explanation for the form of free volume dependence in dynamics.

We start by assuming the basic expression for thermally activated processes, where the relaxation rate is proportional to the Boltzmann factor, $\exp[-E_{act}/T]$, and E_{act} is the activation energy. Though important at high T ,^{25,26} we ignore the gas kinetic $T^{1/2}$ prefactor. The log of the relaxation time ($\tau \propto 1/\text{rate}$) goes as

$$\ln(\tau/\tau_{ref}) = E_{act}/T \quad (4)$$

where τ_{ref} is a constant. Note that E_{act} is the only part of the Boltzmann factor that can be changing with system volume at fixed T . Therefore, connecting eq 4 with the observation (Figure 3) that $\ln \tau$ vs $1/V_{free}$ is linear on isotherms means that the activation energy must be proportional to $1/V_{free}$. The CFV model can explain why this is so.

The CFV model assumes that the relaxation process is both thermally activated and cooperative. This is analogous to the entropy-based approach of Adam and Gibbs.⁵⁴ However, with CFV the degree of the cooperativity is dictated by free volume. For relaxation to occur, molecular segments must cooperate, redistributing (or “donating”) their own free volume, to open up enough free space to allow the entry (or passage) of another segment. Each added cooperating segment brings an added energetic cost (Δa) to the relaxation process, and so the total activation energy is $E_{act} = n^* \Delta a$, where n^* is the number of cooperating segments. n^* is expected to increase in high density conditions where little free volume is available.

The key to how n^* depends, functionally, on V_{free} comes from the expectation (assumption) that the amount of free space needed to allow the full passage of a molecular segment (denoted v^*) must be a characteristic constant of the material, independent of the T, P conditions. Given that each segment in a total system of N segments is capable of donating an amount, V_{free}/N , which will depend on P and T , this leads to a cooperating group size of $n^* = v^*/(V_{free}/N)$. Thus, the CFV model predicts $E_{act} \propto n^* \propto 1/V_{free}$. Because $\ln \tau$ goes as E_{act}/T , this explains why an isothermal plot of $\ln \tau$ vs $1/V_{free}$ is linear.

Next, the result, $E_{act} = n^* \Delta a \propto (1/V_{free}) \times \Delta a$, is inserted into eq 4, which leads to

$$\ln(\tau/\tau_{ref}) = n^* \times \left(\frac{\Delta a(T)}{T} \right) = \left(\frac{1}{V_{free}} \right) \times f(T) \quad (5)$$

This equation matches the general $\ln(\tau/\tau_{ref}) \propto g(V) \times f(T)$ form. We emphasize the importance of the result that the T -

based contribution, $f(T)$, and the V -based contribution, $g(V) \propto 1/V_{free}$, are multiplicatively coupled, which is important for several reasons. First, it explains why the slopes of linear $\ln \tau$ vs $1/V_{free}$ isotherms depend on the isotherm temperature. The slope goes as $f(T) \propto \Delta a(T)/T$, and the simplest approximation of constant Δa in eq 5 leads to the prediction that isotherms are linear and have slopes that increase with decreasing T , which is indeed the qualitative behavior observed in Figure 3.

A second effect explained by the eq 5 multiplicative coupling of T, V contributions is the behavior on isobars. As noted in the discussion of Figure 4, the isobaric plot of $\ln \tau$ vs $1/V_{free}$ has upward curvature. This is because the instantaneous slope at any particular value of $1/V_{free}$ is equal to the $f(T)$ at the corresponding T , so as volume (thus V_{free}) changes along the isobar with T , so does $f(T)$, which causes the ever-increasing slope. Note that if the T and V contributions were only additively coupled (such as in the T, V_{free} -based model of Macedo and Litovitz⁵⁵), then the isobaric $\ln \tau$ vs $1/V_{free}$ plot would not be predicted to show this observed curvature, nor would isotherms be predicted to change slopes.

By similar arguments, the eq 5 form also explains why there is upward curvature in an isobaric plot of $\ln \tau$ vs $1/T$. Again, if we assume a constant Δa for simplicity of argument (constant Δa is actually sufficient over a regime at higher T), then the $\ln \tau$ vs $1/T$ plot has a slope that is proportional to $1/V_{free}$. The experimentally observed increasing slope (viz., the activation energy, E_{act}) reflects the continual increase of $1/V_{free}$ because it is increasing together with $1/T$ along the isobar. The contribution from changing V_{free} therefore explains a fundamental source of non-Arrhenius behavior (fragility^{8,15}) observed in glassy systems.

The form of eq 5, viz., $\ln(\tau/\tau_{ref}) \propto g(V) \times f(T)$, also accounts for the influence of interfaces on glassy dynamics.²⁹ This so-called nanoconfinement effect has attracted considerable research attention.^{4,12,56–67} Though interfaces can lead to a diverse range of observed effects, our analysis^{28,29,68} shows that the interfacial effect can be treated as mostly an effect on the $g(V)$ function; for a free surface, this yields an environment of lowered average density around the segments located near the interface. We have shown that the same T -dependent functional form, $f(T)$, can be used to analyze the behavior of material in the interfacial region (e.g., an ultrathin polymer film) as for that material's bulk dynamics behavior. This explains why shifts in dynamic relaxation for samples of decreasing film thickness (decreasing average density) can be described by a scaling relationship that is analogous to that which captures the relaxation shifts for bulk samples studied under conditions of decreasing pressure.²⁹ Note further that the multiplicative $g(V) \times f(T)$ form also predicts and explains why dynamic sensitivity to changes in film thickness or bulk sample pressure becomes less consequential at higher temperatures, because in this limit $f(T)$ approaches zero.

Before moving on from eq 5 to introduce an empirical form for the T -dependence, we emphasize that the key part of the CFV model is its eq 5 result, $\ln(\tau/\tau_{ref}) \propto (1/V_{free}) \times (\Delta a(T)/T)$. Regardless of the details of the T dependence, the new, and most important, insights from CFV are that it provides a molecular level explanation for how and why the $1/V_{free}$ form captures the system volume dependence, and that it predicts the volume and temperature contributions to relaxation dynamics to be coupled by this multiplicative form. The simple eq 5 result explains how the V -dependence relates to activation energies and, as a result, it is able to predict the

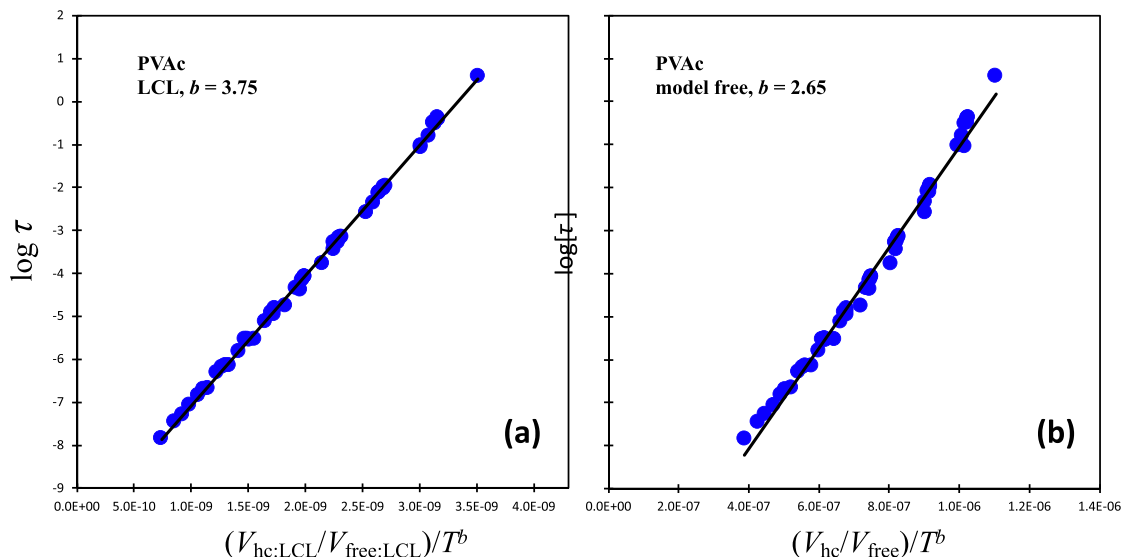


Figure 5. Data collapse of T,P -dependent α -relaxation times for poly(vinyl acetate) (PVAc). Plots show $\log \tau$ vs $(V_{\text{hc}}/V_{\text{free}})/T^b$ (units $1/\text{K}^b$), where the scaling exponent b is applied to describe the T -dependent contribution leading to collapse of the pressure-dependent $\tau(T,V)$ data into a single line; see eq 6. In the left panel (a), free volume defined from previous work and denoted $V_{\text{free:LCL}}$ is calculated from eq 1 using $V_{\text{LCL}}(T,P)$ and $V_{\text{hc:LCL}}$ values from the fitted LCL EOS (parametrization details are available in ref 24). In the right panel (b), free volume from the present work (denoted simply as V_{free}) is calculated from eq 1 based on $V(T,P)$ values from the fitted Tait EOS and where V_{hc} is defined by the linearly extrapolated $V(T = 0, P = 200 \text{ MPa})$ plus a 3% correction (the “best value” in Table 1).

observed qualitative trends resulting from the coupled T and V contributions. This is the first explanation of its kind; the key $\ln \tau \sim f(T) \times (1/V_{\text{free}})$ trends of dynamics shown in Figures 2 and 3 could not have been recognized in the prior literature, in which data analysis had relied on less meaningful (and phenomenological) definitions of V_{free} .

To apply the results of eq 5, we must specify the T -dependence, which appears in that equation in the form $[\Delta a(T)/T]$. (The form of the volume dependence will be unchanged). As noted above, if we make the simplest possible assumption, which is that Δa is constant (no empirical T -dependence), eq 5 with a gas kinetic $T^{1/2}$ prefactor will lead to a quantitative description of pressure-dependent dynamics over the higher T range in the Arrhenius–nonArrhenius crossover regime.^{25,26} However, we aim for a quantitative description of pressure-dependent dynamics data in the T regime of fully super-Arrhenius behavior.

With the form of the V_{free} dependence unchanged, we consider the energy of activation per cooperating segment, $\Delta a(T)$ in eq 5, to be described using an empirical T -dependent form such that $f(T) \sim \Delta a(T)/T \sim 1/T^b$. The material specific scaling exponent b is somewhat analogous to the scaling of V in density scaling approaches.^{1,2,69–77} The result is a simple working expression given by

$$\ln \tau = \left(\frac{V_{\text{hc}}}{V_{\text{free}}} \right) \left(\frac{T^*}{T} \right)^b + \ln \tau_{\text{ref}} \quad (6)$$

Three of the material-specific parameters, b , T^* , and τ_{ref} are determined from system dynamics data. (b can also be determined from $T_g(P)$ from PVT data.) On the other hand, as we have emphasized throughout, V_{hc} and thus all the values for $V_{\text{free}}(T,P) = V(T,P) - V_{\text{hc}}$ are determined solely from *a priori* analysis of *thermodynamic* (PVT) data.

5.3. Application and Comparison of Model-Free and LCL-Based Free Volume. Using the LCL EOS definition for free volume, we have shown that eq 6 is very effective in fitting

and predicting experimental relaxation times, $\tau(T,P)$. In refs 24 and 31 we cover applications to most of the systems in Figure 3, including analyses connecting the CFV model with the density scaling approach. In the comparisons that follow we will denote the LCL-based free volume as “ $V_{\text{free:LCL}}$ ” ($= V_{\text{LCL}}(T,P) - V_{\text{hc:LCL}}$) to distinguish it from the present definition (that requires PVT data but not a theoretical equation of state) which here we simply denote as “ V_{free} ”.

An example of the LCL-based application of CFV eq 6 to PVAc is shown in Figure 5a. (LCL characterization details for PVAc are available in ref 24, $V_{\text{hc:LCL}} = 0.7583 \text{ mL/g}$.) According to eq 6, with the correct system-dependent value for b , a plot of $\ln \tau$ vs $(1/V_{\text{free}})/T^b$ will collapse the system’s T,P -dependent data to yield a single line. The quality of the collapse demonstrates that eq 6 applies very well when LCL-based free volumes are used.

Moving to Figure 5b, the collapse of the data shows that eq 6 also applies, at least roughly, to the present work’s V_{free} values derived from model-free PVT analysis for V_{hc} although the collapse is not quite as tight as when using the $V_{\text{free:LCL}}$ values based on LCL. Cheng et al.⁵³ tested eq 6 on TPIL using V_{free} values extracted from fits to dynamics that are very close to our present model-free values predicted from PVT data (as noted in section 4). They found these V_{free} values yielded an eq 6 collapse that was a bit more scattered than via the consistent LCL analysis, although they did not show the latter; it is included here in the SI. Together the two sets of results for TPIL look analogous to what Figure 5 reveals for PVAc.

In this work both definitions for V_{free} are based on the same simple picture of free volume being measured relative to the close-packed state (eq 1), both are derived solely from thermodynamic measurements (analysis of PVT data), and both lead to $\ln \tau \sim f(T) \times (1/V_{\text{free}})$ behavior. In reading the literature it is important to keep in mind that free volume definitions abound, with most involving fitting quantities or functions that depend on dynamics measurements, and so care

must be taken in making comparisons.²³ The present model-free V_{free} definition has several advantages: It is simple, pedagogically, it provides a very clear connection to dynamics, and at high pressures it maintains a more accurate mapping to the experimental $V(T,P)$ data than $V_{\text{LCL}}(T,P)$ (the latter having an accuracy limited roughly between $P = 1$ atm and 150 MPa). While the model-free V_{free} does not fit eq 6 as tightly as $V_{\text{free:LCL}}$, Figure 5b still shows an impressive collapse. If an even tighter line is the goal, then one could consider modifying eq 6 by adding an additional adjustable parameter to the empirical $f(T)$ function. This will, however, come at the cost of adding a phenomenological parameter without leading to any increase in predictive power or insight.

Because the most predictive power is generally achieved by keeping the adjustable parameters at a minimum, the use of eq 6 with the simple $f(T) \sim 1/T^b$ together with $V_{\text{free:LCL}}$ offers the double advantage of using the simplest possible expression for τ while maintaining the closest possible quantitative agreement with the dynamics data. Furthermore, application of the $V_{\text{free:LCL}}$ definition offers the ability to predict the γ parameter. γ is a key system parameter associated with the density scaling formalism, such that analysis of relaxation dynamics data make use of the single variable via TV^γ .^{1,2,69–77} (In simple analyses γ is often taken as a constant, i.e., the best average value, though other analyses may apply more detailed definitions.^{78–80}) The value of γ has been shown to be connected to a number of important thermodynamic properties,^{76,77,81–86} and for experimental systems, it can be obtained via LCL-CFV with less experimental dynamics data than would be required via the usual density scaling analysis.^{24,31}

6. SUMMARY AND CONCLUSIONS

For decades it was believed that the connection between dynamics and free volume could be described by the Doolittle equation. There was even a corresponding theoretical derivation of this equation in the highly cited work by Cohen and Turnbull.¹⁹ However, when free volume values are based on actual thermodynamic data, the behavior that the Doolittle equation predicts is not followed. Rather, dynamics show a basic $\ln \tau \sim f(T) \times (1/V_{\text{free}})$ behavior. Isotherms of $\ln \tau$ vs $1/V_{\text{free}}$ are linear, but their slopes change with temperature. In addition, $\ln \tau$ vs $1/V_{\text{free}}$ on the standard *ambient pressure isobar* (as well as on isobars at higher P) is not linear as Doolittle predicts but show upward curvature. The CFV rate model predicts the observed behavior using a simple mechanistic framework. Its key assumptions, that the dynamics are thermally activated, and that segmental cooperativity (thus E_{act}) is dependent on free volume, are physical and sensible.

Key to this new insight has been the use of free volume, which we quantify using the locally correlated lattice (LCL) equation of state and solve for by analyzing experimental PVT data. In this paper we offer another, even simpler, definition for free volume, one that works independently of any equation of state. We determine $V_{\text{free}}(T,P) = V(T,P) - V_{\text{hc}}$ based on direct model-free linear extrapolation of PVT data to obtain the closed packed volume, V_{hc} .

We demonstrate here that the $V_{\text{free}}(T,P)$ values obtained by this direct analysis of PVT data serve as a natural variable for analyzing the temperature and pressure dependence of structural relaxation times measured via dielectric spectroscopy, $\tau(T,P)$. This mirrors our previous findings using LCL to define free volume and serves to emphasize that thermody-

namically based free volume plays an important, physically meaningful, role in dynamic relaxation.

Without regard to whether it is determined via an equation of state, or directly from experimental data, it is clear that the importance of system volume in effecting dynamic change is meaningfully captured using V_{free} . As a result of its success in analyzing dielectric relaxation data, accounting for V_{free} explains the origin of non-Arrhenius behavior observed at standard conditions (ambient P) and is critical to explaining the changes to dynamics that can be induced by pressurization and by interfaces.

■ ASSOCIATED CONTENT

SI Supporting Information

The Supporting Information is available free of charge at <https://pubs.acs.org/doi/10.1021/acs.jpcb.1c01620>.

Linear isobaric $V(T)$ data fits for model-free V_{hc} values of all experimental systems; details on Tait EOS analysis of PVT data; TPIL dynamics data collapse for LCL-based free volumes (PDF)

■ AUTHOR INFORMATION

Corresponding Author

Jane E. G. Lipson – Department of Chemistry, Dartmouth College, Hanover, New Hampshire 03755, United States;  orcid.org/0000-0002-0177-9373; Email: jane.lipson@dartmouth.edu

Author

Ronald P. White – Department of Chemistry, Dartmouth College, Hanover, New Hampshire 03755, United States

Complete contact information is available at: <https://pubs.acs.org/10.1021/acs.jpcb.1c01620>

Notes

The authors declare no competing financial interest.

■ ACKNOWLEDGMENTS

J.E.G.L. is pleased to have this opportunity for acknowledging the numerous important contributions of Professor Carol Hall during her long and successful career. Her scientific contributions have advanced areas ranging from computational methods, to phase transitions in fluid mixtures, to self-assembly and structural organization, and more. However, it is equally important to recognize another mechanism by which Carol Hall's legacy will be longstanding: Her warm and effective mentorship and support of junior colleagues, especially women and minority scientists. This author has been the grateful beneficiary of Carol's interest and wisdom and is delighted to recognize with deep thanks the truly important role in her own career that Carol's feedback and support have played. J.E.G.L. and R.P.W. acknowledge financial support from the National Science Foundation through grants DMR-1708542 and DMR-2006504. We also thank Simone Napolitano for providing helpful comments on the manuscript.

■ REFERENCES

- (1) Roland, C.; Hensel-Bielowka, S.; Paluch, M.; Casalini, R. Supercooled Dynamics of Glass-Forming Liquids and Polymers under Hydrostatic Pressure. *Rep. Prog. Phys.* **2005**, *68* (6), 1405–1478.

(2) Floudas, G.; Paluch, M.; Grzybowski, A.; Ngai, K. *Molecular Dynamics of Glass-Forming Systems - Effects of Pressure*; Springer: Berlin, 2011.

(3) Roland, C. M. Relaxation Phenomena in Vitrifying Polymers and Molecular Liquids. *Macromolecules* **2010**, *43* (19), 7875–7890.

(4) Napolitano, S.; Glynn, E.; Tito, N. B. Glass Transition of Polymers in Bulk, Confined Geometries, and near Interfaces. *Rep. Prog. Phys.* **2017**, *80* (3), 036602–036602.

(5) Cangialosi, D. Dynamics and Thermodynamics of Polymer Glasses. *J. Phys.: Condens. Matter* **2014**, *26* (15), 153101–153101.

(6) Dyre, J. C. Colloquium: The Glass Transition and Elastic Models of Glass-Forming Liquids. *Rev. Mod. Phys.* **2006**, *78* (3), 953–972.

(7) Debenedetti, P. G.; Stillinger, F. H. Supercooled Liquids and the Glass Transition. *Nature* **2001**, *410* (6825), 259–267.

(8) Angell, C. Formation of Glasses from Liquids and Biopolymers. *Science* **1995**, *267* (5206), 1924–1935.

(9) Ediger, M.; Angell, C.; Nagel, S. Supercooled Liquids and Glasses. *J. Phys. Chem.* **1996**, *100* (31), 13200–13212.

(10) Angell, C.; Ngai, K.; McKenna, G.; McMillan, P.; Martin, S. Relaxation in Glassforming Liquids and Amorphous Solids. *J. Appl. Phys.* **2000**, *88* (6), 3113–3157.

(11) Berthier, L.; Biroli, G. Theoretical Perspective on the Glass Transition and Amorphous Materials. *Rev. Mod. Phys.* **2011**, *83* (2), 587–645.

(12) Baschnagel, J.; Varnik, F. Computer Simulations of Supercooled Polymer Melts in the Bulk and In-Confinement. *J. Phys.: Condens. Matter* **2005**, *17* (32), R851–R953.

(13) Caruthers, J. M.; Medvedev, G. A. Quantitative Model of Super-Arrhenian Behavior in Glass Forming Materials. *Phys. Rev. Mater.* **2018**, *2* (5), 055604.

(14) McKenna, G. B.; Simon, S. L. Challenges in the Dynamics and Kinetics of Glass-Forming Polymers. *Macromolecules* **2017**, *50*, 6333–6361.

(15) Martinez, L. M.; Angell, C. A. A Thermodynamic Connection to the Fragility of Glass-Forming Liquids. *Nature* **2001**, *410* (6829), 663–667.

(16) Doolittle, A. K. Studies in Newtonian Flow. 2. the Dependence of the Viscosity of Liquids on Free-Space. *J. Appl. Phys.* **1951**, *22* (12), 1471–1475.

(17) Williams, M. L.; Landel, R. F.; Ferry, J. D. Mechanical Properties of Substances of High Molecular Weight. 19. the Temperature Dependence of Relaxation Mechanisms in Amorphous Polymers and Other Glass-Forming Liquids. *J. Am. Chem. Soc.* **1955**, *77* (14), 3701–3707.

(18) Ferry, J. D. *Viscoelastic Properties of Polymers*, 2nd ed.; Wiley: New York, 1970.

(19) Cohen, M. H.; Turnbull, D. Molecular Transport in Liquids and Glasses. *J. Chem. Phys.* **1959**, *31* (5), 1164–1169.

(20) Vogel, H. The Temperature Dependence Law of the Viscosity of Fluids. *Phys. Z.* **1921**, *22*, 645–646.

(21) Fulcher, G. S. Analysis of Recent Measurements of the Viscosity of Glasses. *J. Am. Ceram. Soc.* **1925**, *8* (6), 339–355.

(22) Tammann, G.; Hesse, W. The Dependancy of Viscosity on Temperature in Hypothermic Liquids. *Z. Anorg. Allg. Chem.* **1926**, *156* (4), 245.

(23) White, R. P.; Lipson, J. E. G. Polymer Free Volume and Its Connection to the Glass Transition. *Macromolecules* **2016**, *49* (11), 3987–4007.

(24) White, R. P.; Lipson, J. E. G. The Cooperative Free Volume Rate Model for Segmental Dynamics: Application to Glass-Forming Liquids and Connections with the Density Scaling Approach. *Eur. Phys. J. E: Soft Matter Biol. Phys.* **2019**, *42* (8), 100.

(25) White, R. P.; Lipson, J. E. G. Explaining the T,V-Dependent Dynamics of Glass Forming Liquids: The Cooperative Free Volume Model Tested against New Simulation Results. *J. Chem. Phys.* **2017**, *147* (18), 184503–184503.

(26) White, R. P.; Lipson, J. E. G. Pressure-Dependent Dynamics of Polymer Melts from Arrhenius to Non-Arrhenius: The Cooperative Free Volume Rate Equation Tested against Simulation Data. *Macromolecules* **2018**, *51* (13), 4896–4909.

(27) White, R. P.; Lipson, J. E. G. How Free Volume Does Influence the Dynamics of Glass Forming Liquids. *ACS Macro Lett.* **2017**, *6* (5), 529–534.

(28) White, R. P.; Lipson, J. E. G. Connecting Pressure-Dependent Dynamics to Dynamics under Confinement: The Cooperative Free Volume Model Applied to Poly(4-Chlorostyrene) Bulk and Thin Films. *Macromolecules* **2018**, *51* (20), 7924–7941.

(29) White, R. P.; Lipson, J. E. G. To Understand Film Dynamics Look to the Bulk. *Phys. Rev. Lett.* **2020**, *125*, 058002. DOI: [10.1103/PhysRevLett.125.058002](https://doi.org/10.1103/PhysRevLett.125.058002)

(30) Lipson, J. E. G.; White, R. P. Connecting Theory and Experiment To Understand Miscibility in Polymer and Small Molecule Mixtures. *J. Chem. Eng. Data* **2014**, *59* (10), 3289–3300.

(31) White, R. P.; Lipson, J. E. G. Cooperative Free Volume Rate Model Applied to the Pressure-Dependent Segmental Dynamics of Natural Rubber and Polyurea. *Rubber Chem. Technol.* **2019**, *92* (4), 612–624.

(32) Yi, Y.; Zoller, P. An Experimental and Theoretical-Study of the PVT Equation of State of Butadiene and Isoprene Elastomers to 200-Degrees-C and 200-Mpa. *J. Polym. Sci., Part B: Polym. Phys.* **1993**, *31* (7), 779–788.

(33) Zoller, P.; Walsh, D. *Standard Pressure-Vol.-Temperature Data for Polymers*; Technomic Pub Co.: Lancaster, PA, 1995.

(34) Heinrich, W.; Stoll, B. Dielectric Investigation of the Glass Relaxation in Polyvinyl Acetate) and Polyvinyl-Chloride) Under High Hydrostatic-Pressure. *Colloid Polym. Sci.* **1985**, *263* (11), 873–878.

(35) Roland, C.; Casalini, R. Temperature and Volume Effects on Local Segmental Relaxation in Poly(vinyl acetate). *Macromolecules* **2003**, *36* (4), 1361–1367.

(36) Casalini, R.; Roland, C. Dynamic Properties of Polyvinylmethylether near the Glass Transition. *J. Chem. Phys.* **2003**, *119* (7), 4052–4059.

(37) Ougizawa, T.; Dee, G. T.; Walsh, D. J. Pressure Volume Temperature Properties and Equations of State in Polymer Blends - Characteristic Parameters in Polystyrene Poly(vinyl methyl-ether) Mixtures. *Macromolecules* **1991**, *24* (13), 3834–3837.

(38) Paluch, M.; Roland, C.; Pawlus, S. Temperature and Pressure Dependence of the Alpha-Relaxation in Polymethylphenylsiloxane. *J. Chem. Phys.* **2002**, *116* (24), 10932–10937.

(39) Paluch, M.; Casalini, R.; Patkowski, A.; Pakula, T.; Roland, C. Effect of Volume Changes on Segmental Relaxation in Siloxane Polymers. *Phys. Rev. E: Stat. Phys., Plasmas, Fluids, Relat. Interdiscip. Top.* **2003**, *68* (3), 031802–031802.

(40) Paluch, M.; Pawlus, S.; Roland, C. Pressure and Temperature Dependence of the Alpha-Relaxation in Poly(methyltolylsiloxane). *Macromolecules* **2002**, *35* (19), 7338–7342.

(41) Panagos, P.; Floudas, G. Dynamics of Poly(Propyl Methacrylate) as a Function of Temperature and Pressure. *J. Non-Cryst. Solids* **2015**, *407*, 184–189.

(42) Ortiz-Serna, P.; Diaz-Calleja, R.; Sanchis, M. J.; Floudas, G.; Nunes, R. C.; Martins, A. F.; Visconte, L. L. Dynamics of Natural Rubber as a Function of Frequency, Temperature, and Pressure. A Dielectric Spectroscopy Investigation. *Macromolecules* **2010**, *43* (11), 5094–5102.

(43) Roland, C. M.; Casalini, R. Effect of Hydrostatic Pressure on the Viscoelastic Response of Polyurea. *Polymer* **2007**, *48* (19), 5747–5752.

(44) Casalini, R.; Paluch, M.; Roland, C. M. The Dynamics Crossover Region in Phenol- and Cresol-Phthalein-Dimethylethers under Different Conditions of Pressure and Temperature. *J. Phys.: Condens. Matter* **2003**, *15* (11), S859–S867.

(45) Paluch, M.; Casalini, R.; Best, A.; Patkowski, A. Volume Effects on the Molecular Mobility Close to Glass Transition in Supercooled Phenylphthalein-Dimethylether. II. *J. Chem. Phys.* **2002**, *117* (16), 7624–7630.

(46) Hensel-Bielowka, S.; Ziolo, J.; Paluch, M.; Roland, C. The Effect of Pressure on the Structural and Secondary Relaxations in 1,1'-

Bis(p-Methoxyphenyl) Cyclohexane. *J. Chem. Phys.* **2002**, *117* (5), 2317–2323.

(47) Paluch, M.; Roland, C.; Casalini, R.; Meier, G.; Patkowski, A. The Relative Contributions of Temperature and Volume to Structural Relaxation of van Der Waals Molecular Liquids. *J. Chem. Phys.* **2003**, *118* (10), 4578–4582.

(48) Dlubek, G.; Shaikh, M. Q.; Raetzke, K.; Paluch, M.; Faupel, F. Free Volume from Positron Lifetime and Pressure-Volume-Temperature Experiments in Relation to Structural Relaxation of van Der Waals Molecular Glass-Forming Liquids. *J. Phys.: Condens. Matter* **2010**, *22* (23), 235104.

(49) Casalini, R.; Paluch, M.; Roland, C. Influence of Molecular Structure on the Dynamics of Supercooled van Der Waals Liquids. *Phys. Rev. E: Stat. Phys., Plasmas, Fluids, Relat. Interdiscip. Top.* **2003**, *67* (3), 031505–031505.

(50) Rivera-Calzada, A.; Kaminski, K.; Leon, C.; Paluch, M. Ion Dynamics under Pressure in an Ionic Liquid. *J. Phys. Chem. B* **2008**, *112* (10), 3110–3114.

(51) Paluch, M.; Haracz, S.; Grzybowski, A.; Mierzwa, M.; Pionteck, J.; Rivera-Calzada, A.; Leon, C. A Relationship between Intermolecular Potential, Thermodynamics, and Dynamic Scaling for a Supercooled Ionic Liquid. *J. Phys. Chem. Lett.* **2010**, *1* (6), 987–992.

(52) Cheng, S.; Musial, M.; Wojnarowska, Z.; Holt, A.; Roland, C. M.; Drockenmuller, E.; Paluch, M. Structurally Related Scaling Behavior in Ionic Systems. *J. Phys. Chem. B* **2020**, *124* (7), 1240–1244.

(53) Cheng, S.; Wojnarowska, Z.; Musial, M.; Kolodziej, S.; Drockenmuller, E.; Paluch, M. Studies on Ion Dynamics of Polymerized Ionic Liquids through the Free Volume Theory. *Polymer* **2021**, *212*, 123286.

(54) Adam, G.; Gibbs, J. H. On Temperature Dependence of Cooperative Relaxation Properties in Glass-Forming Liquids. *J. Chem. Phys.* **1965**, *43* (1), 139–146.

(55) Macedo, P. B.; Litovitz, T. A. On Relative Roles of Free Volume and Activation Energy in Viscosity of Liquids. *J. Chem. Phys.* **1965**, *42* (1), 245.

(56) Ediger, M. D.; Forrest, J. A. Dynamics near Free Surfaces and the Glass Transition in Thin Polymer Films: A View to the Future. *Macromolecules* **2014**, *47* (2), 471–478.

(57) Richert, R. Dynamics of Nanoconfined Supercooled Liquids. *Annu. Rev. Phys. Chem.* **2011**, *62*, 65–84.

(58) Alcoutlabi, M.; McKenna, G. Effects of Confinement on Material Behaviour at the Nanometre Size Scale. *J. Phys.: Condens. Matter* **2005**, *17* (15), R461–R524.

(59) Simmons, D. S. An Emerging Unified View of Dynamic Interphases in Polymers. *Macromol. Chem. Phys.* **2016**, *217* (2), 137–148.

(60) Schweizer, K. S.; Simmons, D. S. Progress towards a Phenomenological Picture and Theoretical Understanding of Glassy Dynamics and Vitrification Near Interfaces and under Nanoconfinement. *J. Chem. Phys.* **2019**, *151* (24), 240901.

(61) Phan, A. D.; Schweizer, K. S. Dynamic Gradients, Mobile Layers, T-g Shifts, Role of Vitrification Criterion, and Inhomogeneous Decoupling in Free-Standing Polymer Films. *Macromolecules* **2018**, *51* (15), 6063–6075.

(62) Zhou, Y.; Milner, S. T. Short-Time Dynamics Reveals T-g Suppression in Simulated Polystyrene Thin Films. *Macromolecules* **2017**, *50* (14), 5599–5610.

(63) Cangialosi, D.; Alegria, A.; Colmenero, J. Effect of Nanostructure on the Thermal Glass Transition and Physical Aging in Polymer Materials. *Prog. Polym. Sci.* **2016**, *54*–*55*, 128–147.

(64) Boucher, V. M.; Cangialosi, D.; Yin, H.; Schoenhals, A.; Alegria, A.; Colmenero, J. T-g Depression and Invariant Segmental Dynamics in Polystyrene Thin Films. *Soft Matter* **2012**, *8* (19), 5119–5122.

(65) Fukao, K.; Miyamoto, Y. Glass Transitions and Dynamics in Thin Polymer Films: Dielectric Relaxation of Thin Films of Polystyrene. *Phys. Rev. E: Stat. Phys., Plasmas, Fluids, Relat. Interdiscip. Top.* **2000**, *61* (2), 1743–1754.

(66) Priestley, R. D.; Cangialosi, D.; Napolitano, S. On the Equivalence between the Thermodynamic and Dynamic Measurements of the Glass Transition in Confined Polymers. *J. Non-Cryst. Solids* **2015**, *407*, 288–295.

(67) Kremer, F.; Tress, M.; Mapesa, E. U. Glassy Dynamics and Glass Transition in Nanometric Layers and Films: A Silver Lining on the Horizon. *J. Non-Cryst. Solids* **2015**, *407*, 277–283.

(68) Debot, A.; White, R. P.; Lipson, J. E. G.; Napolitano, S. Experimental Test of the Cooperative Free Volume Rate Model under 1D Confinement: The Interplay of Free Volume, Temperature, and Polymer Film Thickness in Driving Segmental Mobility. *ACS Macro Lett.* **2019**, *8* (1), 41–45.

(69) Casalini, R.; Mohanty, U.; Roland, C. M. Thermodynamic Interpretation of the Scaling of the Dynamics of Supercooled Liquids. *J. Chem. Phys.* **2006**, *125* (1), 014505–014505.

(70) Casalini, R.; Roland, C. M. An Equation for the Description of Volume and Temperature Dependences of the Dynamics of Supercooled Liquids and Polymer Melts. *J. Non-Cryst. Solids* **2007**, *353* (41–43), 3936–3939.

(71) Fragiadakis, D.; Roland, C. M. On the Density Scaling of Liquid Dynamics. *J. Chem. Phys.* **2011**, *134* (4), 044504.

(72) Alba-Simionescu, C.; Cailliaux, A.; Alegria, A.; Tarjus, G. Scaling out the Density Dependence of the a Relaxation in Glass-Forming Polymers. *Europhys. Lett.* **2004**, *68* (1), 58–64.

(73) Guo, J.; Simon, S. L. Thermodynamic Scaling of Polymer Dynamics versus T - T-g Scaling. *J. Chem. Phys.* **2011**, *135* (7), 074901–074901.

(74) Puosi, F.; Chulkov, O.; Bernini, S.; Capaccioli, S.; Leporini, D. Thermodynamic Scaling of Vibrational Dynamics and Relaxation. *J. Chem. Phys.* **2016**, *145* (23), 234904–234904.

(75) Grzybowski, A.; Paluch, M. Universality of Density Scaling. In *The Scaling of Relaxation Processes*; Kremer, F., Loidl, A., Eds.; Advances in Dielectrics; Springer International Publishing: Cham, 2018; pp 77–119. DOI: [10.1007/978-3-319-72706-6_4](https://doi.org/10.1007/978-3-319-72706-6_4).

(76) Dyre, J. C. Hidden Scale Invariance in Condensed Matter. *J. Phys. Chem. B* **2014**, *118* (34), 10007–10024.

(77) Gnan, N.; Schroder, T. B.; Pedersen, U. R.; Bailey, N. P.; Dyre, J. C. Pressure-Energy Correlations in Liquids. IV. “Isomorphs” in Liquid Phase Diagrams. *J. Chem. Phys.* **2009**, *131* (23), 234504.

(78) Bohling, L.; Ingebrigtsen, T. S.; Grzybowski, A.; Paluch, M.; Dyre, J. C.; Schroder, T. B. Scaling of Viscous Dynamics in Simple Liquids: Theory, Simulation and Experiment. *New J. Phys.* **2012**, *14*, 113035.

(79) Casalini, R.; Ransom, T. C. On the Experimental Determination of the Repulsive Component of the Potential from High Pressure Measurements: What Is Special about Twelve? *J. Chem. Phys.* **2019**, *151* (19), 194504.

(80) Casalini, R.; Ransom, T. C. On the Pressure Dependence of the Thermodynamical Scaling Exponent Gamma. *Soft Matter* **2020**, *16* (19), 4625–4631.

(81) Pedersen, U. R.; Bailey, N. P.; Schroder, T. B.; Dyre, J. C. Strong Pressure-Energy Correlations in van Der Waals Liquids. *Phys. Rev. Lett.* **2008**, *100* (1), 015701–015701.

(82) Pedersen, U. R.; Schroder, T. B.; Dyre, J. C. Repulsive Reference Potential Reproducing the Dynamics of a Liquid with Attraction. *Phys. Rev. Lett.* **2010**, *105* (15), 157801–157801.

(83) Coslovich, D.; Roland, C. M. Thermodynamic Scaling of Diffusion in Supercooled Lennard-Jones Liquids. *J. Phys. Chem. B* **2008**, *112* (5), 1329–1332.

(84) Coslovich, D.; Roland, C. M. Pressure-Energy Correlations and Thermodynamic Scaling in Viscous Lennard-Jones Liquids. *J. Chem. Phys.* **2009**, *130* (1), 014508–014508.

(85) Coslovich, D.; Roland, C. M. Density Scaling in Viscous Liquids: From Relaxation Times to Four-Point Susceptibilities. *J. Chem. Phys.* **2009**, *131* (15), 151103.

(86) Casalini, R.; Roland, C. M. Determination of the Thermodynamic Scaling Exponent for Relaxation in Liquids from Static Ambient-Pressure Quantities. *Phys. Rev. Lett.* **2014**, *113* (8), 085701–085701.